A global concept of autocorrelation and power spectral density estimation from LDA data sets

by

H. Nobach

Dantec Measurement Technology
Tonsbakken 16-18, 2740 Skovlunde, Denmark

ABSTRACT

During the last years several advanced algorithms for autocorrelation function (ACF) and power spectral density (PSD) estimation from irregularly sampled LDA data sets have been introduced. The recently performed benchmark tests of spectral estimation from LDA data sets evaluated the performance of several of these techniques and as a result, a recommendation can be made about, which techniques yield most reliable results for given conditions and furthermore, how these techniques can be combined to result in more powerful estimators. Accordingly, the present article introduces a global concept of signal processing from the raw LDA data set to the final ACF and PSD estimates and the estimates of their variability. The entire processing algorithm from the LDA data set to the ACF and PSD estimates consists of the processing steps given in figure below. The details and the purpose of each processing step are described in the article.

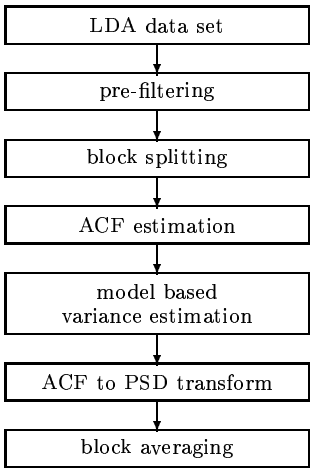

Processing steps of ACF and PSD estimation from LDA data

1. INTRODUCTION

During the last years considerable effort has been made to improve the estimation of the autocorrelation function (ACF) and the power spectral density (PSD) from irregularly sampled LDA data sets. The benchmark tests of spectral estimation from LDA data sets performed by Benedict et al. (1998) evaluated the performance of several of these techniques. Nevertheless, a final set of computational steps describing the optimal method to obtain the ACF and PSD estimations from an LDA data set is still lacking. This article attempts to describe such a procedure, from the raw LDA data set to the final estimations of the ACF and the PSD. Several algorithms, like filtering techniques (Sree et al., 1994, Nobach, 1999a), refined sample-and-hold reconstruction (Nobach et al., 1998b), slot-correlation with fuzzy slotting technique and local normalization by van Maanen et al. (1999) including the use of weighting factors (Nobach, 1999b), model based variance estimation (van Maanen and Tummers, 1996) with some modifications and the block averaging including the estimation of the estimator's variability are discussed.
The following section gives an overview of the processing steps and describes all techniques used in detail. A section with a survey of all influencing parameters of the data processing follows. The final section summarizes the observations.

2. ESTIMATION TECHNIQUE

2.1 Overview

The entire processing algorithm from the LDA data set to the ACF and PSD estimates consists of several processing steps (figure 1). The details and the purpose of each processing step are described in the following subsections.
Important preliminary basics for understanding the following descriptions are as follows:

- The number of values K of the ACF and the temporal resolution $\Delta\tau$ giving the maximum time lag $K\Delta\tau$ are parameters which must be chosen by the user. The maximum time lag inturn determines the resolution Δf of the PSD via the Fourier transform. The block length (block duration, number of samples per block or number of resamples per block after reconstruction) is independent of the maximum time lag of the ACF affects only the variablility of the estimate, to be discussed below.

- The use of smoothing filters is not recommended. Filtering always reduces the information content of the signal and the ACF and the PSD can often be dominated by the filter characteristic. In fact, it is possible to obtain any arbitrary ACF or PSD from any data set by choosing an approprate filter. The fundamental danger of missinterpreting a "good looking" ACF or PSD on the basis of the filter characteristic therefore disqualifies the use of smoothing filters. One exception is the variable windowing technique of Tummers and Passchier (1996). Even this technique produces a falsifying leakage, however due to the frequency dependent scaling of the window it is the same for all frequencies and doesn't lead to an overall distortion of the spectrum.

- The use of zero padding is also not recommended. Normally it is used to augment the number of samples in a record to a power of 2 for using the FFT. One more reason to use this technique is to reduce systematic deviations of the correlation between blocks (wrap around error). The discrete Fourier transform of a time series over a finite number of samples actually computes the amplitude spectrum of the periodically extrapolated signal segment although the true time signal may be quite different. This effect can be reduced by zero padding. But this technique produces other systematic deviations because of the alternation of the time series. Because of the independence of the maximum time lag in the ACF and the block length, the block length can simply be chosen large enough to minimize effects without zero padding. Furthermore, the block length can be chosen in such a way that the number of samples is a power of the base 2. Therefore, the FFT can be used without zero padding.

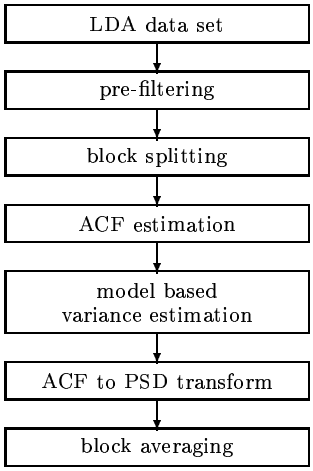

Figure 1: Processing steps of ACF and PSD estimation from LDA data

2.2 Pre-Filtering

To reduce the variability of PSD estimation Sree et al. (1994) used a filtering technique. The same technique can be used to remove a mean velocity or large scale periodicities from an LDA data set. Several filter techniques were investigated by Nobach (1999a) and the possibility of systematic error correction was derived. Nevertheless, the correction procedure is very costly computationally and the basic problem of large time scale uncertainty in the ACF was found. Therefore, the parameters of the filtering technique must be chosen in such a way that the mean velocity and large scale periodicities are removed from the data set with negligible influence on the ACF and the PSD. Then correction procedures are no longer necessary. The symmetric filter used by Nobach (1999a) with a large number of averaged samples, as was also used by Sree et al. (1994), comply with this requirement.
The original LDA velocity samples u_i are averaged to a local mean μ_i

$$\mu_i = \frac{\sum_{j=i-M}^{i+M} u_j w_j}{\sum_{j=i-M}^{i+M} w_j} \tag{1}$$

with a fixed number of samples M on either side and weighting factors w_i to reduce the influence of the velocity bias by appropriate weighting techniques (Fuchs et al., 1994).
To obtain the weighting factors w_i any weighting technique can be used, but the transit time weighting by Hösel and Rodi (1977)

$$w_i = \tau_i \tag{2}$$

under the pre-supposition of high accuracy measurements of the transit time τ_i or the arrival time weighting by Barnet and Bentley (1974)

$$w_i = t_i - t_{i-1} \tag{3}$$

with the arrival time t_i of the velocity sample u_i which is independent of the particle distribution (Fuchs et al., 1994) yield good results.
The pre-filtered velocity sample u_i' is found by

$$u_i' = u_i - \mu_i \tag{4}$$

leading to an LDA data series with the same sampling scheme as the original data set, however with the mean and the large time scale components removed.
To optimize the removal of the mean velocity and of the large scale periodicities with a minimum of systematic errors in the ACF and the PSD the coefficient M is chosen as

$$M \approx K(1 + \dot{n}\Delta\tau) \tag{5}$$

corresponding to the mean data rate $\dot{n}$ and the chosen maximum time lag $K\Delta\tau$ of the ACF.
In the following discussion only filtered data is considered. However the notation u_i is used instead of u_i' for simplicity.

2.3 Block Splitting

Originally the block splitting and averaging technique was introduced by Gaster and Roberts (1977) to reduce the variablility of the direct spectral estimation. With the reconstruction and resampling technique (Adrian and Yao, 1987) the block splitting was used to obtain data records that could be processed conveniently by the FFT. Furthermore, the block length determines the maximum time lag of the ACF and the resolution of the PSD. Increasing the number of blocks for a given LDA data set reduces the variances $\sigma_{\bar{R}}^2$ and $\sigma_{\bar{S}}^2$ of the averaged ACF and PSD estimates respectively.

$$\sigma_{\bar{R}}^2 \sim \frac{1}{N_\mathrm{B}} \tag{6}$$

$$\sigma_{\bar{S}}^2 \sim \frac{1}{N_\mathrm{B}} \tag{7}$$

On the other hand, the FFT computes the PSD of the periodically extrapolated signal as discussed above, leading to systematic errors, especially, for correlation intervals that are greater than the maximum time lag. This puts constraints on making the block length too short.
The slotting technique by Mayo et al. (1974) allows the maximum time lag and the frequency resolution to be chosen independently of any block length by using only a given number K of slots defining the maximum time lag. The variances of the averaged ACF and PSD estimates become

$$\sigma_{\bar{R}}^2 \sim \frac{1}{T_\mathrm{B} N_\mathrm{B}} = \frac{1}{T} \tag{8}$$

$$\sigma_{\bar{S}}^2 \sim \frac{K\Delta\tau}{T_\mathrm{B} N_\mathrm{B}} = \frac{K\Delta\tau}{T} \tag{9}$$

with the block duration T_B and the duration T of the entire data set. This approach can be used as well for the reconstruction techniques described below.
For a given (large) block duration T_B the reconstruction technique refers to a resampled data block with N_R samples at regular time intervals $\Delta\tau$ and a total block duration $T_\mathrm{B} = K\Delta\tau$. The corresponding PSD and the ACF also have N_R samples. Equations (8) and (9) apply also to this estimator using $K\Delta\tau = T_\mathrm{B}$. The variability of the ACF estimation is independent of the maximum time lag. However the PSD estimation depends on the maximum time lag. Reducing the maximum time lag by cutting the ACF at $K\Delta\tau < T_\mathrm{B}$ and recalculating the PSD by the Fourier transform yields a reduced variability of the PSD estimation. Incidently, this is the cause of the low estimation variance of the variable windowing technique from Tummers and Passchier (1996), especially for high frequencies.
For a given K the variability of the ACF estimate depends only on the entire data set length as follows from equations (8) and (9). Therefore, the block splitting can be dispensed with and the entire data set can be processed together. However an estimation of the estimator variance (section 2.7) requires at least 10 blocks and therefore block splitting is often retained. Furthermore, the splitting technique can be helpful in collecting blocks that can be processed by the FFT in connection with the reconstruction and resampling technique. The block length should be large compared to the correlation interval (integral time scale) and at least $2K\Delta\tau$ to reduce end effects. A smaller block length could be implemented for on-line measurements, in order to obtain a general idea of the flow statistics, with larger blocks being used for final measurements to minimize the measurement variance.

2.4 ACF Estimation

In the benchmark tests of spectral estimation from LDA data sets performed by Benedict et al. (1998) the refined reconstruction technique by Nobach et al. (1996) and Nobach et al. (1998b), the slotting technique with the local normalization by van Maanen and Tummers (1996) and the fuzzy slotting technique by Nobach et al. (1998a) were all found to yield good results. The latter two algorithms have since been

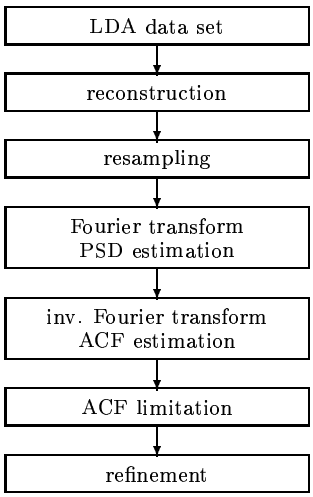

Figure 2: Processing steps of the reconstruction method

combined by van Maanen et al. (1999) to a more powerful estimator. The resulting slotting algorithm and the reconstruction algorithm each have distinctive advantages. While the slotting technique has the smaller variability, the blockwise processing of reconstructed and resampled data is faster, especially for high data densities and furthermore, the given procedure can be extended by the refinement filter of Nobach et al. (1998b) very easily. Both algorithms are described in detail in the following sections.
Reconstruction. The widely used reconstruction method for ACF and PSD estimation consists of:

- the reconstruction of the continuous velocity signal from the LDA samples,
- the equidistant resampling,
- the PSD estimation using the Fourier transform and
- the ACF estimation using the inverse Fourier transform.

To obtain improved results this procedure was extended by (figure 2):

- the limitation to a maximum time lag independent of the block length and
- the refinement filter.

The advantage of this technique is the small influence of any mean velocity bias, because after the reconstruction the particle velocity values with large interarrival times are resampled more often than values with smaller interarrival times. This principle is similar to the arrival time weighting by Buchhave et al. (1979) used in moment estimation.
To obtain the continuous velocity signal from the LDA samples the sample-and-hold reconstruction (zero-order polynomial)

$$u'(t) = u_i \qquad \text{for } t_i \le t < t_{i+1} \text{ and } i = 1 \ldots N \tag{10}$$

is widely used, where N is the total number of samples in a given block. The reconstruction can be carried out over the entire data set or with single data blocks. Other reconstruction techniques have been investigated and the results, including the correction of the particle-rate filter, are similar. Therefore, the sample-and-hold reconstruction is sufficient and furthermore, the refinement filter becomes very simple only for this reconstruction scheme.
The equidistant resampling with time steps of $\Delta\tau$ performed by

$$u'_i = u'(i\Delta\tau) \qquad \text{for } i = 0 \ldots N_\mathrm{R} - 1 \tag{11}$$

leads to a data set that can be processed by the FFT if the number of resamples within one block N_R is a power of 2. The FFT

$$U'_j = \sum_{i=0}^{N_R-1} u'_i e^{-2\pi i j i/N_R} \quad \text{for } j = 0 \ldots N_R - 1 \tag{12}$$

leads to the full block PSD

$$\hat{S}'_j = \frac{\Delta\tau}{N_R} \left|U'_j\right|^2 \quad \text{for } j = 0 \ldots N_R - 1 \tag{13}$$

and through the inverse FFT

$$X'_k = \frac{1}{N_R} \sum_{j=0}^{N_R-1} \hat{S}'_j e^{2\pi j k i/N_R} \qquad \text{for } k = 0 \ldots N_R - 1 \tag{14}$$

to the full block ACF

$$\hat{R}'_k = \frac{1}{\Delta\tau} X'_k \qquad \text{for } k = 0 \ldots N_R - 1. \tag{15}$$

The ACF to PSD transform (section 2.6) uses $K+1$ values ($k = 0 \ldots K$). The refinement filter requires one more value, so that $K+2$ values ($k = 0 \ldots K+1$) of the block ACF are used for the refinement. In the case of the sample-and-hold reconstruction the refinement filter becomes a simple FIR-filter (Nobach et al., 1998b)

$$\hat{R}_k = \begin{cases} \hat{R}'_0 & \text{for } k = 0 \\ (2c+1)\hat{R}'_k - c\left(\hat{R}'_{k-1} + \hat{R}'_{k+1}\right) & \text{for } k = 1 \ldots K \end{cases} \tag{16}$$

with the filter parameter

$$c = \frac{e^{-\dot{n}\Delta\tau}}{\left(1 - e^{-\dot{n}\Delta\tau}\right)^2} \tag{17}$$

depending only on the mean particle rate $\dot{n}$. The refined ACF $\hat{R}_k$ is used in the subsequent processing steps.

Slot Correlation. To reduce the variability of the original slotting algorithm by Mayo et al.(1974) the local normalization by van Maanen and Tummers (1996) and the fuzzy slotting technique by Nobach et al. (1998a) were combined by van Maanen et al. (1999) to a more powerful algorithm. Additionally, the algorithm was extended by Nobach (1999b) using weighting algorithms known from the estimation of statistical values like the mean velocity or the variance (Fuchs et al., 1994). The advantage of this algorithm is the very low variability and the possibility of reducing the influence of the velocity bias by several weighting techniques.

Every combination of two samples u_i and u_j within a block taken at the times t_i and t_j is processed for each time lag $k\Delta\tau$ using

$$\hat{R}_k = \frac{\hat{\sigma}_u^2 A}{\sqrt{BC}} \qquad \text{for } k = 0 \ldots K \tag{18}$$

with

$$A = \sum_{i=1}^{N-1} \sum_{j=i+1}^{N} u_i u_j w_i w_j b_k(t_j - t_i) \tag{19}$$

$$B = \sum_{i=1}^{N-1} \sum_{j=i+1}^{N} u_i^2 w_i w_j b_k(t_j - t_i) \tag{20}$$

$$C = \sum_{i=1}^{N-1} \sum_{j=i+1}^{N} u_j^2 w_i w_j b_k(t_j - t_i) \tag{21}$$

with the weighting factors w_i and the fuzzy mask function

$$b_k(\Delta t) = \begin{cases} 1 - \left|\frac{\Delta t}{\Delta\tau} - k\right| & \text{for } \left|\frac{\Delta t}{\Delta\tau} - k\right| < 1 \\ 0 & \text{otherwise} \end{cases} \tag{22}$$

and the velocity variance

$$\hat{\sigma}_u^2 = \frac{\sum_{i=1}^{N} u_i^2 w_i}{\sum_{i=1}^{N} w_i}. \tag{23}$$

To obtain the weighting factors the same procedures as those for the local mean in the pre-filtering section 2.2 can be used, but in the case of an arrival time weighting the foreward-backward weighting introduced by Nobach (1999b)

$$w_i = t_i - t_{i-1} \tag{24}$$

$$w_j = t_{j+1} - t_j \tag{25}$$

should be employed, because of the correlation between the time lag and the arrival time distribution.

2.5 Model Based Noise Removal/Variance Estimation

The value $\hat{R}_0$ of the ACF at time lag zero is obscured by various effects. Because of the unused self-products, the slotting technique (section 2.4) is independent of noise in the LDA data. However the processor delay distorts the results. The reconstruction algorithm (section 2.4) is sensitive to the noise in the LDA data and the processor delay.
To remove the noise and the effect of the processor delay from the ACF estimate, a model-based estimation of $\hat{R}_0$ can be used. Principally speaking, convenient models like those of van Maanen and Oldenziel (1998) or Müller et al. (1998) can be used. Nevertheless, the parameter optimization is difficult and costly. The use of a weighting function with larger coefficients close to the time lag zero allows simpler models to be used. As a model of the ACF van Maanen and Tummers (1996) used a Gaussian function, corresponding to the Taylor microscale estimation. Good results were obtained using the more flexible model

$$R_k = ae^{-bk^c}, \tag{26}$$

which is equivalent to the Gaussian function for $c = 2$ and to the exponential function for $c = 1$. Nevertheless, even this model is not able to describe periodic components, so that the weighting function should decrease very strongly with the time lag τ, i.e. $1/\tau$ or similar. The figure of merit

$$d = \sum_{k=1}^{K} k^{-1}(\hat{R}_k - R_k)^2 \tag{27}$$

gives the weighted deviation of the model ACF R_k to the estimated ACF $\hat{R}_k$. Note that the value $\hat{R}_0$ is not used because of its dominating on d. Minimizing the figure of merit d leads to an optimal parameter set $[a; b; c]$.
The optimum of the amplitude a can be expressed explicitly as the solution of

$$\frac{\mathrm{d}\, d}{\mathrm{d}\, a} = 0 \tag{28}$$

leading to

$$a = \frac{\sum_{k=1}^{K} k^{-1}\hat{R}_k e^{-bk^c}}{\sum_{k=1}^{K} k^{-1}e^{-2bk^c}} \tag{29}$$

The derivation can be found in the appendix.
The optimum of the parameter b has to be found iteratively with the tangent algorithm

$$b_{n+1} = b_n - \frac{\frac{\mathrm{d}\, d}{\mathrm{d}\, b}}{\frac{\mathrm{d}^2 d}{\mathrm{d}\, b^2}} \tag{30}$$

and the argument b_n for the derivatives (see appendix).
The procedure starts for a given c with the initial parameter $b = 0$. Only values with $a > 0$, $b > 0$ are accepted and the convexity of $d(b)$ is checked after each iteration step through

$$\frac{\mathrm{d}^2 d}{\mathrm{d}\, b^2} > 0 \tag{31}$$

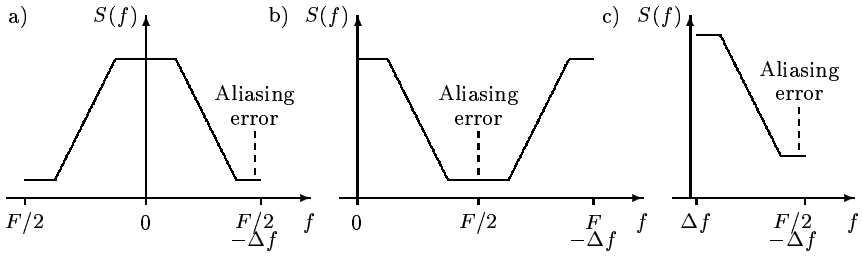

Figure 3: Different spectrum representations: a) symmetric to zero; b) symmetric to $F/2$ and c) only for positive frequencies

Approximately 10 iteration steps are necessary to reach an accuracy of 10^{-6} for the parameter b. This is necessary to preserve the correct relation between the results for different values of the parameter c.
The iteration has to be repeated for several values of c, starting with $c = 0.1$ and steps of 0.1, yielding for the parameter c to a resolution of 10^{-1}. This describes the ACF precisely enough. That parameter c is taken as an optimum that leads to the smallest final value d after the iteration without any failure. In the case of success the model-based value $R_0 = a$ is taken as the new ACF estimate at time lag zero.

2.6 Transform

From the ACF estimation (section 2.4) a set of $K + 1$ values ($k = 0 \ldots K$) is obtained. Because of the symmetry of the ACF, it can be expanded to the symmetric ACF with $2K$ values ($k = -K \ldots K - 1$) through

$$\hat{R}_k = \hat{R}_{-k} \qquad \text{for } k = -K \ldots -1. \tag{32}$$

so that a power of 2 results. The corresponding PSD is

$$\hat{S}_j = \Delta\tau \sum_{k=-K}^{K-1} \hat{R}_k \cos\left(\frac{2\pi jk}{2K}\right) \qquad \text{for } j = -K \ldots K-1 \tag{33}$$

which is symmetric about zero (figure 3a). It is defined between $-F/2$ and $F/2 - \Delta f$ with $F = 1/\Delta\tau$ and $\Delta f = F/2K$ with an aliasing error at the edges.
The limitation of the frequency range is important to preserve the demand

$$\hat{R}_0 = \Delta f \sum_j S_j \tag{34}$$

Because of the possibility of calculating equation (33) for any j leading to a periodic function, the PSD is often represented between 0 and $F - \Delta f$, symmetric about $F/2$ (figure 3b), with the aliasing error close to $F/2$. A third widely used representation is the result of a harmonic analyze, which cannot differ between positive and negative frequencies. That leads to the superposition $S_j + S_{-j}$ of the PSD parts. Because of the symmetry of the PSD, this gives the doubled PSD value (figure 3c). Note that this is possible for frequencies between 0 and $F/2$ only.
The FFT algorithm requires a data set that is numbered from 0 to $2K - 1$ with a symmetry at K. Therefore another expansion of the ACF is necessary.

$$\hat{R}_k = \hat{R}_{2K-k} \qquad \text{for } k = K \ldots 2K-1. \tag{35}$$

The FFT of this data set yields

$$X_j = \sum_{k=0}^{2K-1} \hat{R}_k \cos\left(\frac{2\pi jk}{2K}\right) \qquad \text{for } j = 0 \ldots 2K-1 \tag{36}$$

and the PSD is

$$\hat{S}_j = \Delta\tau X_j \qquad \text{for } j = 0 \ldots 2K-1 \tag{37}$$

corresponding to the PSD representation in figure 3b. This can be transfered to the other representations. Alternatively to the use of the FFT with the full ACF estimate, Tummers and Passchier (1996) recommended a frequency dependent variable windowing of the ACF for the transform to the PSD

$$\hat{S}(f) = \Delta\tau \sum_{k=-K}^{K-1} \hat{R}_k w_k \cos(2\pi f k \Delta\tau) \tag{38}$$

corresponding to the PSD representation in figure 3b. Good experience was obtained using the Tuckey-Hanning window with

$$w_k = \begin{cases} \frac{1}{2} + \frac{1}{2}\cos\left(\frac{\pi k f \Delta\tau}{\kappa}\right) & \text{for } |kf\Delta\tau| < \kappa \\ 0 & \text{otherwise} \end{cases} . \tag{39}$$

The parameter κ can be chosen arbitrarily, eg. $\kappa = 6$ was found to give good results.
This technique reduces the estimation variance especially for higher frequencies, while through the windowing a leakage effect arises. However now the spectrum can be calculated at any frequency. This could reduce the number of required spectral lines in the case of a logarithmic axis scaling which is often used to present turbulence spectra. This is important because the the FFT cannot be used for this transform and every spectral value has to be calculated independently.

2.7 Block Averaging

Each block of LDA data leads to an independent ACF and PSD estimate. For N_B blocks the mean ACF $\bar{R}$, the mean PSD $\bar{S}$ and the corresponding variances σ_R^2 and σ_S^2 of the single block estimates can be calculated using

$$\bar{R} = \frac{1}{N_\mathrm{B}} \sum_{i=1}^{N_\mathrm{B}} \hat{R}^{(i)} \tag{40}$$

$$\bar{S} = \frac{1}{N_\mathrm{B}} \sum_{i=1}^{N_\mathrm{B}} \hat{S}^{(i)} \tag{41}$$

$$\sigma_R^2 = \frac{1}{N_\mathrm{B} - 1} \sum_{i=1}^{N_\mathrm{B}} (\hat{R}^{(i)} - \bar{R})^2 \tag{42}$$

$$\sigma_S^2 = \frac{1}{N_\mathrm{B} - 1} \sum_{i=1}^{N_\mathrm{B}} (\hat{S}^{(i)} - \bar{S})^2 \tag{43}$$

where the upper index (i) represents the estimates of the i-th block. The variance of the averaged ACF and PSD can be estimated through

$$\sigma_{\bar{R}}^2 = \frac{1}{N_\mathrm{B}} \sigma_R^2 \tag{44}$$

$$\sigma_{\bar{S}}^2 = \frac{1}{N_\mathrm{B}} \sigma_S^2 \tag{45}$$

The mean and variance estimates (equations 40–43) can be calculated recursively through

$$\bar{R}^{(n)} = \frac{R^{(n)} + (n-1)\bar{R}^{(n-1)}}{n} \tag{46}$$

$$\bar{S}^{(n)} = \frac{S^{(n)} + (n-1)\bar{S}^{(n-1)}}{n} \tag{47}$$

$$(\sigma_R^2)^{(n)} = \frac{1}{n-1}\left[(R^{(n)})^2 - n(\bar{R}^{(n)})^2 + (n-1)(\bar{R}^{(n-1)})^2 + (n-2)(\sigma_R^2)^{(n-1)}\right] \tag{48}$$

$$(\sigma_S^2)^{(n)} = \frac{1}{n-1}\left[(S^{(n)})^2 - n(\bar{S}^{(n)})^2 + (n-1)(\bar{S}^{(n-1)})^2 + (n-2)(\sigma_S^2)^{(n-1)}\right] \tag{49}$$

for each new block n from the preceding estimates.

3. PROCESSING PARAMETERS

Beside the option of data processing algorithm (weighting algorithm, reconstruction or slotcorrelation), several operating parameters must be prescribed.
For the parameter M of the pre-filtering algorithm, $M \approx \dot{n} K \Delta\tau$ was given already in section 2.2.
The temporal resolution $\Delta\tau$ can be chosen independently of the data rate $\dot{n}$. However to prevent effects of the processor delay on the ACF estimates $\hat{R}_k$ at $k > 0$ it should not be chosen smaller than the processor delay. Furthermore, the variability of the ACF estimation and thus the variability of the PSD are indirectly proportional to $\Delta\tau$. Therefore, the time step $\Delta\tau$ should not be chosen much smaller than the mean time between particle arrivals corresponding to the data rate $\dot{n}$, i.e. $1/\Delta\tau \leq 10\dot{n}$.
The number of ACF values K is independent of the block length. It can be chosen in a wide range, but it should be a power of 2 to enable the use of the FFT. In that case the frequency resolution of the PSD becomes

$$\Delta f \sim \frac{1}{K} \tag{50}$$

placing a practical limit on how small K should be. Good experience was made with values of 64–1024. The block length T_B should be chosen to be at least $2K\Delta\tau$, better $10K\Delta\tau$, to prevent effects of the block edges on the ACF estimate. The estimation of the estimation's variability (section 2.7) needs at least 10 blocks for a reliable result. The mean ACF and PSD estimation already work with only one block. Depending on the purpose of the measurement the block length could be defined differently. A smaller block length could be prefered for on-line measurements to obtain a general idea of the flow statistics and larger blocks for final measurements to maximize the measurement accuracy.

4. CONCLUSIONS

The described procedure to obtain estimates of the ACF and the PSD from an LDA data set combines several powerful alorithms. The implemented algorithms are found to be very robust for many practical measurement conditions. The number and the meaning of processing parameters to be chosen are easily understood even for a user that is not very familiar with the theory of signal processing. This article summarizes a global concept of signal processing with all required formulae for successful implementation in a program.

ACKNOWLEDGMENT

The author wishes to acknowledge the financial support of the Deutsche Forschungsgemeinschaft through the grants Tr 194/9, Mu 1117/1 and No 373/1.

REFERENCES

Adrian, R. J. and Yao, C. S. (1987). "Power spectra of fluid velocities measured by laser Doppler velocimetry", Exp. in Fluids, 5:17–28

Barnet, D. O. and Bentley, H. T. (1974). "Statistical bias of individual realization laser velocimetry", In Proc. 2nd Int. Workshop on Laser Velocimetry, pp 428–444, Purdue

Benedict, L. H., Nobach, H. and Tropea, C. (1998). "Benchmark tests for the estimation of power spectra from LDA signals", In Proc. 9th Int. Symp. on Appl. of Laser Techn. to Fluid Mechanics, Lisbon, Portugal, paper 32.6.

Benedict, L. H., Nobach, H. and Tropea, C. (2000). "Estimation of turbulent velocity spectra from laser Doppler data", Meas. Sci. Technol., 11 (August 2000)

Buchhave, P., George Jr, W. K. and Lumley, J. L. (1979). "The measurement of turbulence with the laser Doppler anemometer", In Annual Review of Fluid Mechanics, volume 11, pp 442–503, Annual Reviews,

Inc., Palo Alto, CA

Fuchs, W., Nobach, H. and Tropea, C. (1994). "Laser Doppler anemometry data simulation: Application to investigate the accuracy of statistical estimators", AIAA Journal, 32:1883–1889

Gaster, M. and Roberts, J. B. (1977). "The spectral analysis of randomly sampled records by a direct transform", Proc. R. Soc. Lond. A., 354:27–58

Hösel, W. and Rodi, W. (1977). "New biasing elimination method for laser-Doppler-velocimeter counter processing", Rev. Sci. Instrum., pp 910–919

Mayo Jr, W. T., Shay, M. T. and Ritter, S. (1974). "The development of new digital data processing techniques for turbulence measurements with a laser velocimeter", AEDC-TR-74-53

Mc Laughlin, D. K. and Tiederman, W. G. (1973). "Biasing correction for individual realisation of laser anemometer measurements in turbulent flows", Phys. of Fluids, 16(12):2082–2088

Müller, E., Nobach H. and Tropea, C. (1998). "Model parameter estimation from non-equidistant sampled data sets at low data rates", Meas. Sci. Technol., 9(3):435–441

Nobach H. (1999a). "LDA data filtering", Technical report, Technische Universität Darmstadt, Fachbereich Maschinenbau, Fachgebiet Strömungslehre und Aerodynamik, Report No. 007/1999

Nobach H. (1999b). "Processing of stochastic sampled data in laser Doppler anemometry", In Proc. 3rd International Workshop on Sampling Theory and Applications, pp 149–154

Nobach, H., Müller, E. and Tropea, C. (1996). "Refined reconstruction techniques for LDA data analysis", In Proc. 8th Int. Symp. on Appl. of Laser Techn. to Fluid Mechanics, Lisbon, Portugal, paper 36.2.

Nobach, H., Müller, E. and Tropea, C. (1998a). "Correlation estimator for two-channel, non-coincidence laser-Doppler-anemometer", In Proc. 9th Int. Symp. on Appl. of Laser Techn. to Fluid Mechanics, Lisbon, Portugal, paper 32.1.

Nobach, H., Müller, E. and Tropea, C. (1998b). "Efficient estimation of power spectral density from laser Doppler anemometer data", Experiments in Fluids, 24:499–509

Sree, D., Kjelgaard, S. O. and Sellers III, W. L. (1994). "Spectral enhancement of randomly sampled signals by pre-filtering techniques", Laser Anemometry — 1994: Advances and Applications, pp 680–685, ASME 1994, FED-Vol. 191

Tummers, M. J. and Passchier, D. M. (1996). "Spectral estimation using a variable window and the slotting technique with local normalization", Meas. Sci. Technol., 7:1541–1546

van Maanen, H. R. E., Nobach, H. and Benedict, L. H. (1999). "Improved estimator for the slotted autocorrelation function of randomly sampled LDA data", Meas. Sci. Technol., 10(1):L4–L7

van Maanen, H. R. E. and Oldenziel, A. (1998). "Estimation of turbulence power spectra from randomly sampled data by curve-fit to the autocorrelation function applied to laser-Doppler anemometry", Meas. Sci. Technol., 9:458–467

van Maanen, H. R. E. and Tummers, M. J. (1996). "Estimation of the autocorrelation function of turbulent velocity fluctuations using the slotting technique with local normalization", In Proc. 8th Int. Symp. on Appl. of Laser Techn. to Fluid Mechanics, Lisbon, Portugal, paper 36.4.

DERIVATIVES OF THE ACF MODEL

The ACF model is

$$R_k = ae^{-bk^c} = aE \tag{51}$$

with the substitution

$$E = e^{-bk^c} \tag{52}$$

The figure of merit is

$$d = \sum_{k=1}^{K} k^{-1} (\hat{R}_k - aE)^2, \tag{53}$$

which has to be minimized.
The derivative with respect to a is

$$\frac{\mathrm{d}\, d}{\mathrm{d}\, a} = \sum_{k=1}^{K} 2k^{-1}(aE - \hat{R}_k)E = 2a\sum_{k=1}^{K} k^{-1}E^2 - 2\sum_{k=1}^{K} k^{-1}\hat{R}_k E \tag{54}$$

The constraint of equation (28) leads to

$$a = \frac{\sum_{k=1}^{K} k^{-1}\hat{R}_k E}{\sum_{k=1}^{K} k^{-1}E^2} = \frac{Z}{N} \tag{55}$$

with the notation

$$Z = \sum_{k=1}^{K} k^{-1}\hat{R}_k E \tag{56}$$

$$N = \sum_{k=1}^{K} k^{-1}E^2 \tag{57}$$

corresponding to equation (29).
In the following the amplitude is a function of the parameter b. It follows

$$\frac{\mathrm{d}\, a}{\mathrm{d}\, b} = \frac{N\frac{\mathrm{d}\, Z}{\mathrm{d}\, b} - Z\frac{\mathrm{d}\, N}{\mathrm{d}\, b}}{N^2} \tag{58}$$

$$\frac{\mathrm{d}^2 a}{\mathrm{d}\, b^2} = \frac{N^2\frac{\mathrm{d}^2 Z}{\mathrm{d}\, b^2} - 2N\frac{\mathrm{d}\, Z}{\mathrm{d}\, b}\frac{\mathrm{d}\, N}{\mathrm{d}\, b} - ZN\frac{\mathrm{d}^2 N}{\mathrm{d}\, b^2} + 2Z\left(\frac{\mathrm{d}\, N}{\mathrm{d}\, b}\right)^2}{N^3} \tag{59}$$

with

$$\frac{\mathrm{d}\, Z}{\mathrm{d}\, b} = \sum_{k=1}^{K} k^{-1}\hat{R}_k \frac{\mathrm{d}\, E}{\mathrm{d}\, b} \tag{60}$$

$$\frac{\mathrm{d}^2 Z}{\mathrm{d}\, b^2} = \sum_{k=1}^{K} k^{-1}\hat{R}_k \frac{\mathrm{d}^2 E}{\mathrm{d}\, b^2} \tag{61}$$

$$\frac{\mathrm{d}\, N}{\mathrm{d}\, b} = \sum_{k=1}^{K} 2k^{-1}E\frac{\mathrm{d}\, E}{\mathrm{d}\, b} \tag{62}$$

$$\frac{\mathrm{d}^2 N}{\mathrm{d}\, b^2} = \sum_{k=1}^{K} 2k^{-1}\left[\left(\frac{\mathrm{d}\, E}{\mathrm{d}\, b}\right)^2 + E\frac{\mathrm{d}^2 E}{\mathrm{d}\, b^2}\right] \tag{63}$$

$$\frac{\mathrm{d}\, E}{\mathrm{d}\, b} = -k^c E \tag{64}$$

$$\frac{\mathrm{d}^2 E}{\mathrm{d}\, b^2} = k^{2c} E \tag{65}$$

For the figure of merit d follows

$$\frac{\mathrm{d}\, d}{\mathrm{d}\, b} = 2\sum_{k=1}^{K} k^{-1}(aE - \hat{R}_k)\left(\frac{\mathrm{d}\, a}{\mathrm{d}\, b}E + a\frac{\mathrm{d}\, E}{\mathrm{d}\, b}\right) \tag{66}$$

$$\frac{\mathrm{d}^2 d}{\mathrm{d}\, b^2} = 2\sum_{k=1}^{K} k^{-1}\left[(aE - \hat{R}_k)\left(\frac{\mathrm{d}^2 a}{\mathrm{d}\, b^2}E + 2\frac{\mathrm{d}\, a}{\mathrm{d}\, b}\frac{\mathrm{d}\, E}{\mathrm{d}\, b} + a\frac{\mathrm{d}^2 E}{\mathrm{d}\, b^2}\right) + \left(\frac{\mathrm{d}\, a}{\mathrm{d}\, b}E + a\frac{\mathrm{d}\, E}{\mathrm{d}\, b}\right)^2\right]. \tag{67}$$